Analysis of Fast Bipedal Walking Using Mechanism of Actively Controlled Wobbling Mass

Yuta Hanazawa, Terumitsu Hayashi, Masaki Yamakita and Fumihiko Asano

Dept. of Mechanical and Control Engineering, Kyushu Institute of Technology, 1-1 Sensui, Tobata, Kitakyushu, Fukuoka 804-8550, JAPAN.

E-mail: hanazawa@cntl.kyutech.ac.jp

Yaskawa denki Co., 2-1 Kurosaki-siroishi, Yahata-nishi, Kitakyushu, Fukuoka 806-0004, JAPAN.

E-mail: hayashi@ac.ctrl.titech.ac.jp

Dept. of Mechanical and Control Engineering, Tokyo Institute of Technology, 2-12-1 Oh-okayama, Meguro-ku Tokyo 152-8552, JAPAN.

E-mail: yamakita@ac.ctrl.titech.ac.jp

School of Information Science, Japan Advanced Institute of Science and Technology, 1-1 Asahidai, Nomi, Ishikawa 923-1292, JAPAN.

E-mail: fasano@jaist.ac.jp

Abstract. In this study, a novel approach was developed to achieve fast bipedal walking by using an actively controlled wobbling mass. Bipedal robots capable of achieving energy efficient limit cycle walking have been developed, and researchers have studied methods to increase their walking speed. When humans walk, their arm swinging is coordinated with the walking phases, generating a regular symmetrical motion about the torso. The bipedal robots with a wobbling mass in the torso were mimicked the arm swinging by the proposed control method. We demonstrated that the proposed method is capable of increasing the bipedal walking speed.

Keywords: Biped robot, Wobbling mass, Limit cycle walking

1. INTRODUCTION

Bipedal walkers can flexibly change their walking direction, even in confined spaces, and can traverse a wide range of terrains. This study aimed to apply these desirable characteristics to a bipedal robot that is capable of achieving fast and energy efficient dynamic walking. Several researchers have developed bipedal walkers that can traverse uneven terrains or climb stairs [1], [2]. Over the last decade, considerable progress has also been made in the area of improving the energy efficiency of bipedal robots. One approach has applied passive dynamic walking [3], which is also known as limit cycle walking (LCW) [4]. Limit cycle walkers use their own dynamics to achieve more energy efficient walking in comparison with the competing designs [4]. However, they are slower than many other bipedal robots such as ASIMO, and researchers have attempted to find ways of improving this.

Asano et al. demonstrated fast LCW by incorporating designs with arc-shaped feet [5], and a parametric-excitation mechanism [6]. The effects of these leg mechanism consequently generated highly efficient and fast bipedal walking. Banno et al. demonstrated fast LCW using a parametric-excitation mechanism with knee and used it in a robot of their design [7]. Hobbelen et al. demonstrated LCW using ankle spring [8], which have excellent effects similar to those of semicircular feet, and allowing energy efficient and fast dynamic walking. They have also demonstrated walking speed control of an LCW robot whose upper-body posture allowed fast walking to be achieved [8]. Hanazawa et al. have shown that ankle springs and inerters lend the bipedal robots more appropriate mechanical impedance at their ankles to achieve energy effcient and fast limit cycle walking [9]. They have also demonstrated fast LCW using asymmetric swing leg motions [10] and shown that bipedal robots generate propulsion for dynamic walking when the swing leg motion is synchronized with the stance leg motion. Bao et al. demonstrated that fast LCW could be achieved by utilizing the rhythmic sway of the torso [11].

Therefore, we wanted to develop a novel method achieving fast LCW. We define fast LCW as walking that are faster than many previously actuated limit cycle walkers. Previously developed limit cycle walkers have been demonstrated to walk on level ground at a Froude number of Fr = 0.15 [12]. The Froude number is an index of the walking speed, which is defined as the walking speed divided by the square root of gravity multiplied by the leg length, $v/\sqrt{gl}$.

Rome et al. demonstrated that the walking motions of human subjects carrying heavy backpacks were improved when elastic elements were applied to the backpack's up-and-down movements [13]. Tanaka et al. increased the speed of a combined rimless wheel by using the up-and-down movements of a wobbling mass [14]. It is well known that human achieve level ground walking with the dynamic arm swinging [15]. The instinctive arm-swinging movements made by humans during walking are similar to the up-and-down movements of a wobbling mass when observed from the sagittal plane, as seen in
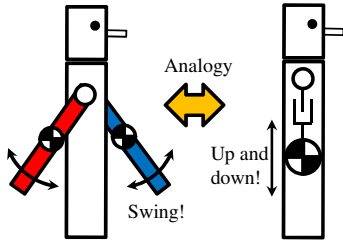
Fig. 1. Analogy between swinging arms and wobbling mass: the left figure shows the robot with arms, and the right figure shows the robot with an actively controlled wobbling mass

Fig. 2. Bipedal robot model with a wobbling mass

Fig. 1. Moreover, we assume a regular pattern of the arm-swinging movements according that matches the walking phase.

Humans change the amplitude of their arm swinging to reflect the walking speed, i.e., a small change is observed when walking slowly, and a larger change is observed when walking quickly. This suggests that the walking speed can be improved by applying actively regular vertical movements to a wobbling mass, partly mimicking the arm-swinging movements of humans. This study propose a novel method on this observation. The effectiveness of the actively controlled wobbling mass is confirmed in this paper.

The rest of this paper is organized as follows. In Section II, a bipedal-robot model is introduced. In Section III, we show an active-control method for a wobbling mass. In Section IV, level-ground walking with a wobbling mass is numerically demonstrated. In Section V, we present the results of our parametrical study on the energy efficiency and walking speed of the robot. In Section VI, we discuss using a spring to the energy-efficiency of the walking. Finally, the paper is concluded in Section VII.

2. MATHEMATICAL MODEL OF ROBOT

2.1. Equation of motion

A bipedal-robot model is shown in Fig. 2. The model has a torso with an actively controlled wobbling mass and arc-shaped feet. The wobbling mass can be increased or decreased through the use of a linear actuator positioned in the torso. There are two additional actuators that control the movement of the torso and swing leg. The equation of motion for the bipedal robot is given as

$$M(q)\ddot{q} + H(q,\dot{q}) = S_1 u + J_c(q)^T \lambda, \quad \ldots \ldots (1)$$

where $q = [\theta_1, \ \theta_2, \ \theta_3, \ l_b, \ x_1, \ z_1]^T$ is the generalized coordinate vector, $M(q) \in \mathbb{R}^{6\times6}$ is an inertial matrix, $H(q,\dot{q}) \in \mathbb{R}^6$ is a Coriolis, centrifugal, and gravitational force vector, $u = [u_1, \ u_2, \ u_3]^T$ is an input vector, and the
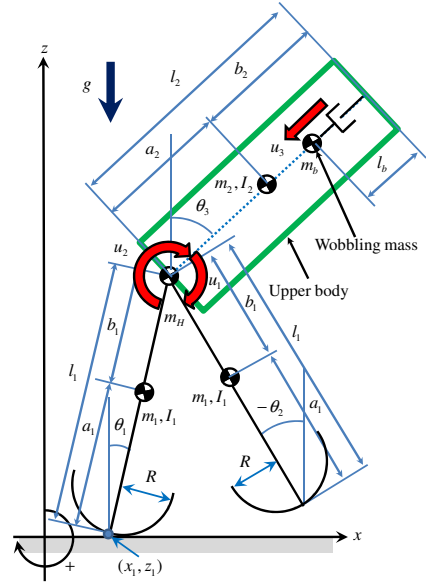
driving matrix $S_1 \in \mathbb{R}^{6\times3}$ is represented as

$$S_1 = \begin{bmatrix} 0 & -1 & 0 \\ 1 & 0 & 0 \\ -1 & 1 & 0 \\ 0 & 0 & 1 \\ 0 & 0 & 0 \\ 0 & 0 & 0 \end{bmatrix} \ldots \ldots \ldots \ldots (2)$$

$J_c(q) \in \mathbb{R}^{N\times6}$ is a Jacobian that is depend on the constraint of the robot, where N is the number of constraint conditions. $\lambda \in \mathbb{R}^N$ is a constraint force vector, which can be obtained by

$$\lambda = -X(q)^{-1}(J_c(q)M(q)^{-1}\Gamma(q,\dot{q},u) + \dot{J}_c(q,\dot{q})\dot{q}), \quad (3)$$

$$X(q) = J_c(q)M(q)^{-1}J_c(q)^T, \quad (4)$$

$$\Gamma(q,\dot{q},u) = S_1 u - H(q,\dot{q}). \quad (5)$$

2.2. Constraint conditions

To analyze the effectiveness of the proposed method, we investigated LCW under the condition of active control of the up-and-down motions in freely movable and physically constrained wobbling mass. We derived $J_c(q)$, $\dot{J}_c(q,\dot{q})$ for each of the following cases.

2.2.1. Freely movable case

Since the bipedal robot's is only in contact with the ground, the constraint equations are expressed as follows:

$$R(\cos\theta_1 - 1)\dot{\theta}_1 + \dot{x}_1 = 0, \quad (6)$$

$$-R\sin\theta_1\dot{\theta}_1 + \dot{z}_1 = 0. \quad (7)$$

From Eqs. (6) and (7), we determined $\boldsymbol{J}_c(\boldsymbol{q}) \in \mathbb{R}^{2 \times 6}$ and $\dot{\boldsymbol{J}}_c(\boldsymbol{q},\dot{\boldsymbol{q}}) \in \mathbb{R}^{2 \times 6}$ as follows:

$$\boldsymbol{J}_c(\boldsymbol{q})\dot{\boldsymbol{q}} = \begin{bmatrix} R(\cos\theta_1 - 1) & 0 & 0 & 0 & 1 & 0 \\ -R\sin\theta_1 & 0 & 0 & 0 & 0 & 1 \end{bmatrix}\dot{\boldsymbol{q}} = \boldsymbol{0}_{2\times1}, \quad (8)$$

$$\dot{\boldsymbol{J}}_c(\boldsymbol{q},\dot{\boldsymbol{q}}) = \begin{bmatrix} -R\dot{\theta}_1\sin\theta_1 & 0 & 0 & 0 & 0 & 0 \\ -R\dot{\theta}_1\cos\theta_1 & 0 & 0 & 0 & 0 & 0 \end{bmatrix}. \quad (9)$$

2.2.2. Physically constrained case

When the wobbling mass is physically constrained (i.e., $l_b = l_0$), we obtained the following constraint equation:

$$\dot{l}_b = 0. \quad \ldots \ldots \ldots \ldots \ldots \ldots \quad (10)$$

Based on Eqs. (6), (7), and (10), $\boldsymbol{J}_c(\boldsymbol{q}) \in \mathbb{R}^{3 \times 6}$ and $\dot{\boldsymbol{J}}_c(\boldsymbol{q},\dot{\boldsymbol{q}}) \in \mathbb{R}^{3 \times 6}$ can be expressed as follows:

$$\boldsymbol{J}_c(\boldsymbol{q})\dot{\boldsymbol{q}} = \begin{bmatrix} R(\cos\theta_1 - 1) & 0 & 0 & 0 & 1 & 0 \\ -R\sin\theta_1 & 0 & 0 & 0 & 0 & 1 \\ 0 & 0 & 0 & 1 & 0 & 0 \end{bmatrix}\dot{\boldsymbol{q}} = \boldsymbol{0}_{3\times1}, \quad (11)$$

$$\dot{\boldsymbol{J}}_c(\boldsymbol{q},\dot{\boldsymbol{q}}) = \begin{bmatrix} -R\dot{\theta}_1\sin\theta_1 & 0 & 0 & 0 & 0 & 0 \\ -R\dot{\theta}_1\cos\theta_1 & 0 & 0 & 0 & 0 & 0 \\ 0 & 0 & 0 & 0 & 0 & 0 \end{bmatrix}. \quad (12)$$

2.3. Impact equation

We assume that contact between each swing leg and the ground is inelastic and instantaneous. The velocity immediately after impact can be derived by solving the impact equations. Additionally, the angles and angular velocities are updated in the simulations.

2.3.1. Freely movable case

For the freely movable wobbling mass, the constraint equations are expressed as follows:

$$l_1 \cos\theta_1 \dot{\theta}_1 + ((R - l_1)\cos\theta_2 - R)\dot{\theta}_2 + \dot{x}_1 = 0, \quad (13)$$

$$-l_1 \sin\theta_1 \dot{\theta}_1 + (l_1 - R)\sin\theta_2 \dot{\theta}_2 + \dot{z}_1 = 0. \quad (14)$$

The instantaneous constraint matrix $\boldsymbol{J}_I(\boldsymbol{q}) \in \mathbb{R}^{2 \times 6}$ is then given by

$$\boldsymbol{J}_I(\boldsymbol{q}) = \begin{bmatrix} A_1 & A_2 & 0 & 0 & 1 & 0 \\ A_3 & A_4 & 0 & 0 & 0 & 1 \end{bmatrix}, \quad \ldots \quad (15)$$

where $A_1 = l_1 \cos\theta_1$, $A_2 = (R - l_1)\cos\theta_2 - R$, $A_3 = -l_1 \sin\theta_1$, and $A_4 = (l_1 - R)\sin\theta_2$.

2.3.2. Physically constrained case

The following constraint equation is applicable under the condition that the wobbling mass is constrained ($l_b = l_0$):
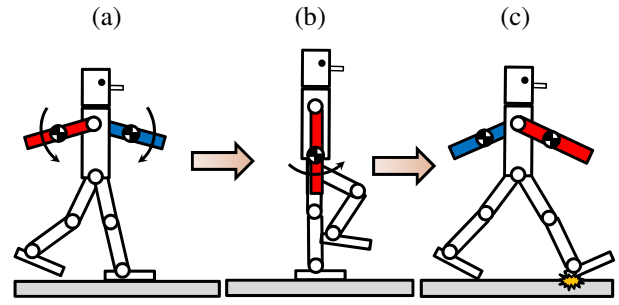
$$\dot{l}_b = 0. \quad \ldots \ldots \ldots \ldots \ldots \ldots \quad (16)$$

Fig. 3. Bipedal walking with active dual-arm movement

From Eqs. (13), (14), and (16), $\boldsymbol{J}_I(\boldsymbol{q}) \in \mathbb{R}^{3 \times 6}$ is given by

$$\boldsymbol{J}_I(\boldsymbol{q}) = \begin{bmatrix} B_1 & B_2 & 0 & 0 & 1 & 0 \\ B_3 & B_4 & 0 & 0 & 0 & 1 \\ 0 & 0 & 0 & 1 & 0 & 0 \end{bmatrix}, \quad \ldots \quad (17)$$

where $B_1 = l_1 \cos\theta_1$, $B_2 = (R - l_1)\cos\theta_2$, $B_3 = -l_1 \sin\theta_1$, $B_4 = (l_1 - R)\sin\theta_2$. The impulsive force vector, $\boldsymbol{\lambda}_I \in \mathbb{R}^N$, and corresponding velocity vector, $\dot{\boldsymbol{q}}^+ \in \mathbb{R}^6$, immediately after the impact are respectively given by

$$\boldsymbol{\lambda}_I = -\boldsymbol{X}_I(\boldsymbol{q})^{-1}\boldsymbol{J}_I(\boldsymbol{q})\dot{\boldsymbol{q}}^-, \quad (18)$$

$$\boldsymbol{X}_I(\boldsymbol{q}) = \boldsymbol{J}_I(\boldsymbol{q})\boldsymbol{M}(\boldsymbol{q})^{-1}\boldsymbol{J}_I(\boldsymbol{q})^{\mathrm{T}}, \quad (19)$$

$$\dot{\boldsymbol{q}}^+ = (\boldsymbol{I} - \boldsymbol{M}(\boldsymbol{q})^{-1}\boldsymbol{J}_I(\boldsymbol{q})^{\mathrm{T}}\boldsymbol{X}_I(\boldsymbol{q})^{-1}\boldsymbol{J}_I(\boldsymbol{q}))\dot{\boldsymbol{q}}^-, \quad (20)$$

where $\dot{\boldsymbol{q}}^- \in \mathbb{R}^6$ is the velocity vector immediately prior to the impact, and N is the number of instantaneous constraint conditions upon impact. We apply Eq. (15) in the case of the freely movable wobbling mass and Eq. (17) in the case of the physically constrained wobbling mass. The bipedal robot changes the stance-leg immediately after the collision of the feet with ground.

3. CONTROL METHOD

3.1. Control for torso and swing-leg

Level ground walking was achieved by applying the following simple partial differential control equations:

$$u_1 = -K_{P1}(\phi_d - (\theta_1 - \theta_2)) - K_{D1}(\dot{\theta}_2 - \dot{\theta}_1), \quad (21)$$

$$u_2 = -K_{P2}(\theta_3 - \theta_{3d}) - K_{D2}\dot{\theta}_3 + u_1, \quad (22)$$

where K_{P1}, K_{P2}, K_{D1} and K_{D2} are the control gains, ϕ_d is the desired hip-joint angle, and θ_{3d} is the desired torso angle. Eq. (21) allows the bipedal robot to raise its swing-leg, whereas Eq. (22) allows it to maintain the desired torso angle.

3.2. Control of the wobbling mass for fast walking

The vertical movement of the wobbling mass was assumed to be analogous to dual arm movement in human walking. Fig. 3 shows bipedal walking with active dual arm movement. The masses of dual arm descend from
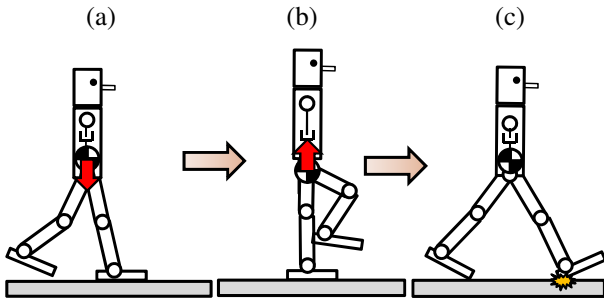
Fig. 4. Bipedal walking with a wobbling mass

4. WALKING ANALYSIS

4.1. Realization of dynamic walking

We present the results of implementing our control method in a numerical simulation. Table 1 lists the physical parameters of the bipedal robot. We empirically determined the control parameters listed in Table 2.

Figs. 5, 6, and 7 show the phase trajectories for level ground walking with an actively wobbling mass. Figs. 8 and 9 show the input torques and force with respect to time for the one gait cycle. Figs. 10, 11, and 12 show the potential energy, kinetic energy and mechanical energy, respectively. It can be seen that the bipedal robot achieved one-period LCW. We next investigated the wobbling movement with respect to the stance leg angle and the vertical movement of the torso mass. Fig. 13 shows the stance leg angle in LCW, Fig. 14 shows the height of the torso, and Fig. 15 shows the height of the wobbling mass relative to the torso mass. The movement of the actively controlled wobbling mass was in antiphase with the vertical movement of the torso. Table 3 show the walking speed under three conditions: no wobbling mass,

their initial position immediately after the collision of the swing leg, and reach the lowest point at the vertical stance leg. Moreover, the mass points then ascend until the next collision of the swing leg. These relationships are not dependent on the walking speed, and humans automatically adjust their arm swings during a gait cycle. Similarly, the amplitude of the vertical wobbling movement of the mass points is also adjusted with the waking speed, i.e., the amplitude is large when the robot is walking fast, and small when it is walking slowly.

As shown in Fig. 4, we therefore treated the serial motion as the actively controlled wobbling motion of the mass. Considering the above-described analysis of human-arm swinging, the mass was setup to immediately descend after the collision of the swing leg (Fig. 4(a)), reaches the lowest point in its trajectory when the angle of the stance leg is vertical (Fig. 4(b)), and ascend until the next collision of the swing leg (Fig. 4(c)). This motion is in antiphase with the vertical motion of the center of mass of the torso, Our proposed method regulates the antiphase motion of the mass using the control input:

$$u_3 = -K_{P3}(l_b - l_{bd}) - K_{D3}(\dot{l}_b - \dot{l}_{bd}), \quad \ldots \ldots (23)$$

where K_{P3} and K_{D3} are the control gains, The desired trajectory function for the wobbling mass l_{bd} is given by

$$l_{bd} := K_a(P_z - d_t) + d_w, \quad \ldots \ldots \ldots \ldots (24)$$

where K_a is the parameter that decides the wobbling amplitude, P_z is the height of the mass point in the torso, and d_t is the desired height of this mass point when the stance leg angle is vertical. In this case, $d_t = l_1 + a_2$, since the torso is always vertical ($\theta_3 = 0$) , and d_w is the parameter that determines the maximum length of l_b. The time differentiation for the desired trajectory is given by

$$\dot{l}_{bd} = K_a(\dot{z}_1 - l_1 \sin\theta_1 \dot{\theta}_1 - a_2 \sin\theta_3 \dot{\theta}_3). \quad \ldots (25)$$

This control almost ensures that the wobbling movement of the mass is in antiphase with that of the torso mass.

Table 1. Physical parameters

Symbol	Value	Unit
l_0	0.25	m
l_1	1.0	m
l_2	1.0	m
$a_1 = b_1 = l_1/2$	0.5	m
$a_2 = b_2 = l_2/2$	0.5	m
R	0.1	m
m_1	5.0	kg
m_2	5.0	kg
m_H	5.0	kg
m_b	2.0	kg
I_1	4.17×10^{-1}	kg· m^2
I_2	4.17×10^{-1}	kg· m^2

Table 2. Control parameters

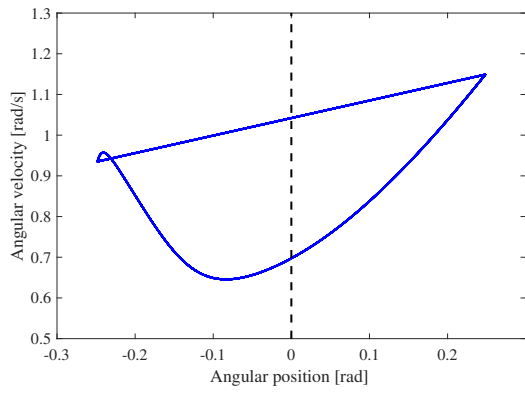| Symbol	Value	Unit
K_{P1}	100	N·m/rad
K_{D1}	25	N·m/(rad/s)
K_{P2}	1000	N·m/rad
K_{D2}	200	N·m/(rad/s)
K_{P3}	1000	N/m
K_{D3}	50	N/m
ϕ_d	0.60	rad
θ_{3d}	0.00	rad
d_t	1.5	m
d_w	0.5	m
K_a	5.0	-

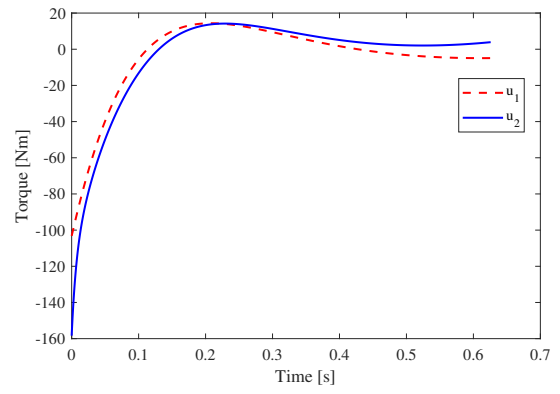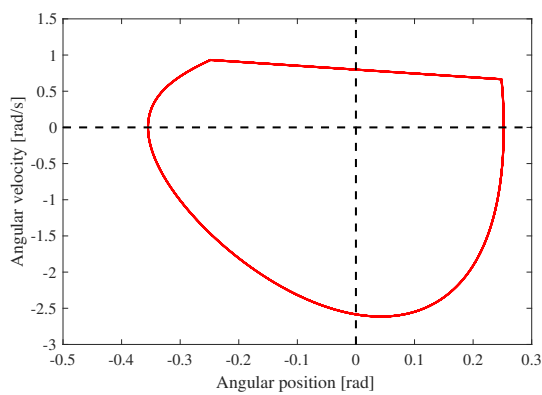**Fig. 5.** Phase trajectories of the stance leg ($\theta_1 - \dot\theta_1$) during LCW with an actively wobbling mass

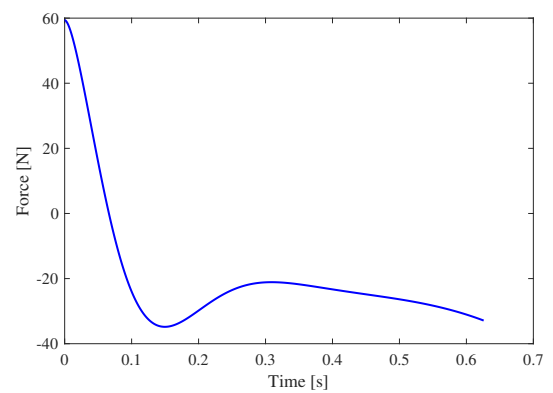**Fig. 6.** Phase trajectories of the swing leg ($\theta_2 - \dot\theta_2$) during LCW with an actively wobbling mass
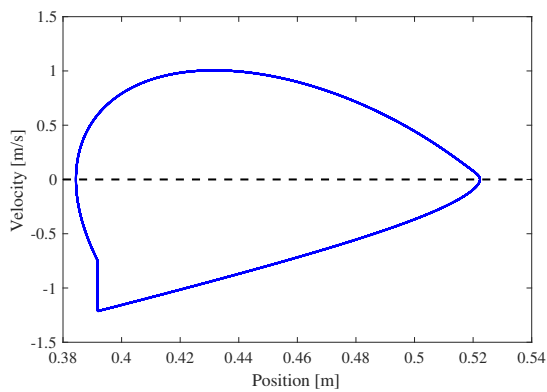

Fig. 7. Phase trajectories of the movement of the actively wobbling mass ($l_b - \dot{l}_b$) during LCW

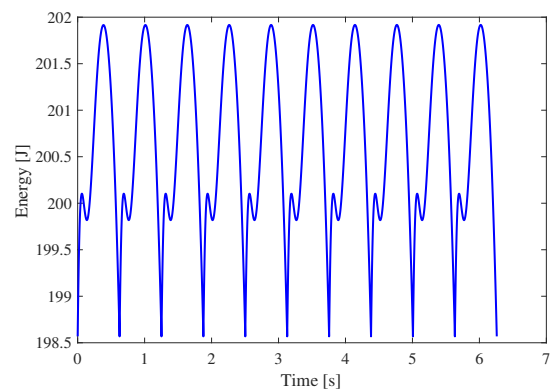**Fig. 8.** u_1 and u_2 with respect to time

Fig. 9. u_3 with respect to time

Fig. 10. Total potential energy during LCW with an actively wobbling mass

with a physically constrained wobbling mass, and with an up-and-down wobbling mass. The fastest walking was achieved when the actively wobbling mass was used, confirming that our proposed method can increase the speed

of bipedal robots. Specifically, the robot with an actively controlled mass achieved considerably fast walking at Fr = 0.25. In the next subsection, we analyze the details of the speed-up mechanism.
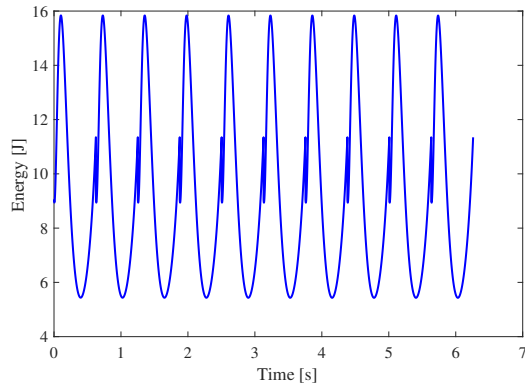
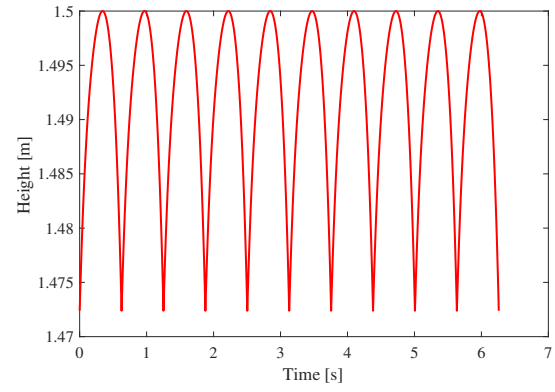**Fig. 11.** Total kinetic energy during LCW with an actively wobbling mass

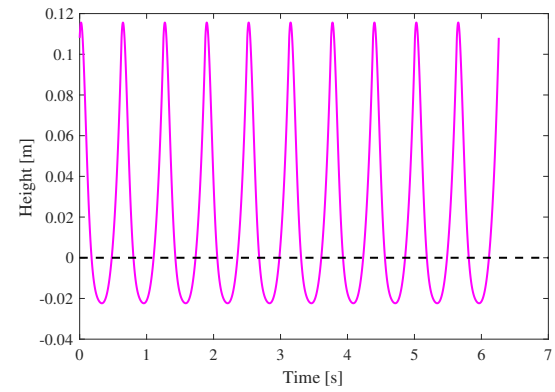**Fig. 12.** Total mechanical energy during LCW with an actively wobbling mass
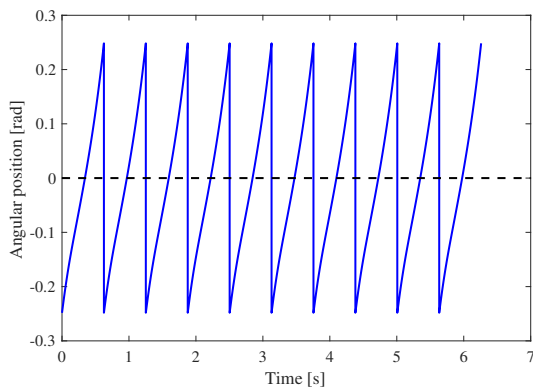

Fig. 13. Stance leg angle during LCW with an actively wobbling mass

4.2. Using the vertical movement of the wobbling mass to improve walking speed

To consider the contribution of the wobbling mass to the reaction force under the conditions of our control

Fig. 14. Height of the mass point of the torso during LCW with an actively wobbling mass

Fig. 15. Relative height of actively wobbling mass during LCW

Table 3. Walking speed under each condition

Condition	Speed
no mass	0.59 m/s
locked mass	0.53 m/s
actively controlled mass	0.79 m/s

method, we defined a position vector from the origin to the torso mass (m_2) as

$$\boldsymbol{p}_t = \begin{bmatrix} x_1 + l_1 \sin\theta_1 + a_2 \sin\theta_3 \\ 0 \\ z_1 + l_1 \cos\theta_1 + a_2 \cos\theta_3 \end{bmatrix}, \quad \ldots \ldots (26)$$

where each x, y and z element of the vector is as shown in Fig. 2. Since our model is planar, the y element of the vector has a value of 0 m. Since the wobbling motions of the mass are dependent on the height of the mass point of the torso, this constitutes the third element of Eq. (26)(i.e., the z element of the vector).

We suppose that the radius of the arc-shaped feet is negligibly small, and that z_1 is negligibly small during dynamic walking. The control input for the torso ensures

that it maintains a nearly vertical posture. Since the torso angle (θ_3) is nearly 0 rad, the following relationship is satisfied:

$$a_2 \cos(\theta_3) \approx a_2 \times 1 = a_2. \quad . \quad . \quad . \quad . \quad . \quad . \quad . \quad (27)$$

Since the height of the wobbling mass is determined by the second term in the third element of Eq. (26), $l_1 \cos \theta_1$, the height of the wobbling mass is dependent on the angle of the stance leg (θ_1). This height monotonically increases over time beginning at the point at which the stance leg changes, and reaching its maximum value when this leg is vertical ($\theta_1 = 0$).

The height then monotonically decreases over time when $\theta_1 > 0$. The control input for the wobbling mass ensures that its up-and-down motion is in antiphase with the torso-mass height, and it generates a reaction force that serves to drive the robot to perform forward dynamic walking when the stance leg angle is negative ($\theta_1 < 0$) as shown in Fig. 16. It also generates a reaction force to produce forward driving effects during dynamic walking when the stance leg angle is positive ($\theta_1 > 0$) as shown in Fig. 17. These reaction forces generate torque around the contact point of the stance leg, which can be described as follows:

$$M = [0\ 1\ 0](\boldsymbol{r} \times \boldsymbol{F}), \quad . \quad . \quad . \quad . \quad . \quad . \quad . \quad . \quad . \quad (28)$$

where $\boldsymbol{r}$ is the position vector from the contact point of the stance leg to the hip joint and $\boldsymbol{F}$ is the reaction force vector generated by the control mechanism. A bipedal robot can be considered to have a virtual actuator at the ankle, which generates the driving torque.

To more clearly elucidate the forward driving effects, we suppose that the stance leg angle (θ_1) monotonically increases through the stance phase. We further suppose that the reaction force induced by the wobbling mass is always positive when the stance leg angle is negative ($\theta_1 < 0$) and negative when this angle is positive ($\theta_1 > 0$). Under these assumptions, the contribution of the torque generated by the virtual actuator at the ankle to the driving effect at the equilibrium point ($\theta_1 \approx 0$) of the mechanical energy can be determined as follows:

$$E = \int_{T_s}^{T_0} \dot{\theta}_1 (-Fl_1\theta_1)\mathrm{d}t + \int_{T_0}^{T_e} \dot{\theta}_1 (Fl_1\theta_1)\mathrm{d}t, \quad . \quad . \quad (29)$$

where T_s is the time immediately after the stance leg changes, T_0 is the time at which the stance leg angle is vertical, and T_e is the time immediately after the collision of the swing leg with the ground. The stance leg angle is negative from T_s to T_0 and positive from T_0 to T_e.

If all assumptions are satisfied, the first term on the right-hand side of Eq. (29) is always positive from T_s to T_0, whereas the second term is always positive from T_0 to T_e. The torque generated by the virtual ankle then transfers the positive mechanical energy to the bipedal robots, propelling it forward. Since these assumptions are mostly satisfied by our proposed control method, the antiphase up-and-down motion effectively increases the LCW speed. Fig. 18 shows that the mechanical energy from T_s to T_e is calculated by Eq. (29). It can be seen that

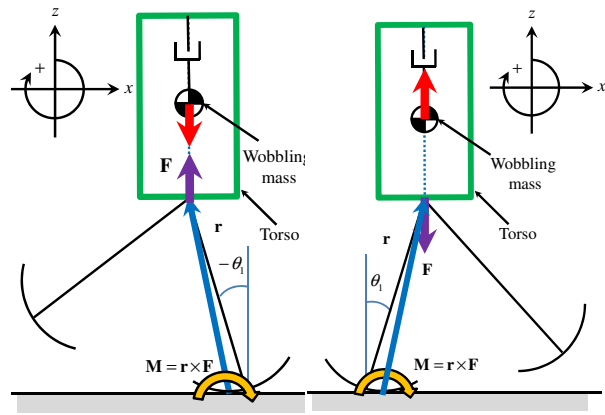**Fig. 16.** $\theta_1 < 0$, i.e., when wobbling mass falls

Fig. 17. $\theta_1 > 0$, i.e., when wobbling mass rises

the effects of the wobbling mass cause the mechanical energy to monotonically increase.

5. PARAMETRIC STUDY

To explore the other elements that affect walking performance, e.g., the size of the wobbling mass, the amplitude of the up-and-down motion, and the arc-radius of the feet, we conducted a parametric study.

5.1. Effects of the size of the wobbling mass

Fig. 19 shows that walking speed monotonically increased as the size of wobbling mass increased. We next investigated the energy-efficiency of the method by using the specific-resistance (SR) as the energy-efficiency index in bipedal robots. The SR is expressed as follows:

$$\mathrm{SR} := \frac{p}{M_t g v}, \quad . \quad . \quad . \quad . \quad . \quad . \quad . \quad . \quad . \quad . \quad (30)$$

where p [J/s] is the average input power, M_t [kg] is the total mass of the robot and v [m/s] is the average walking speed. The average input power, p, is given by

$$p := \frac{1}{T} \int_0^T \left(|u_1(\dot{\theta}_2 - \dot{\theta}_3)| + |u_2(\dot{\theta}_3 - \dot{\theta}_1)| + |u_3 \dot{l}_b| \right) \mathrm{d}t, (31)$$

For example, the SR of the humanoid robot Asimo is 1.6 [4].

Fig. 20 shows the same behaviour for the SR. From these results, we can see that the walking speed and SR increases when the wobbling mass increases: this is because increasing this mass increases the reaction force under the condition of our control method, thereby enhancing the forward driving effects that enable dynamic walking.

5.2. Effects of amplitude of the wobbling movement

The walking speed with respect to the amplitude of movement of the wobbling mass is shown in Fig. 21. The
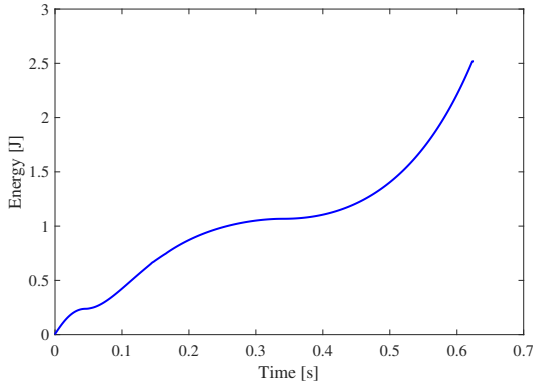
Fig. 18. Mechanical energy generated by wobbling motion during the time period ranging from T_s to T_e
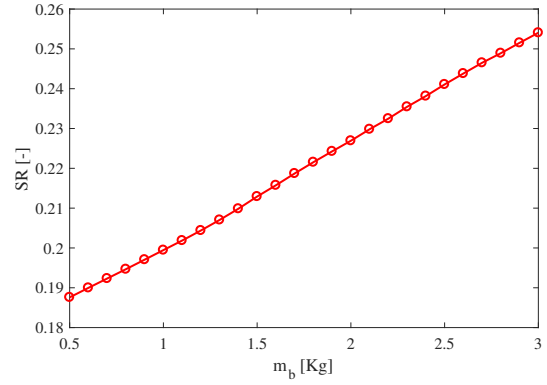

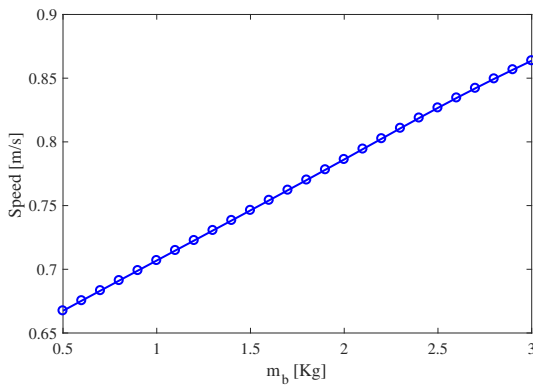**Fig. 20.** SR with respect to wobbling mass

Fig. 19. Walking speed with respect to wobbling mass
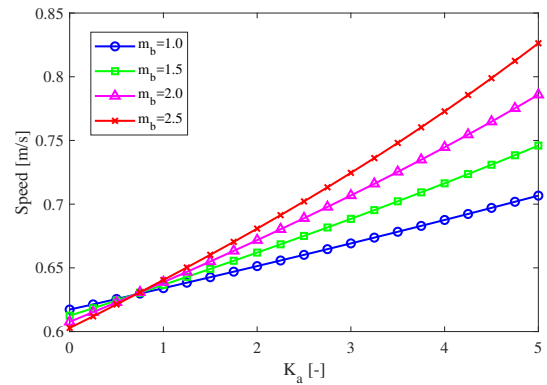

Fig. 21. Walking speed with respect to amplitude of up-and-down motion

speed monotonically increased as the wobbling amplitude increased. Fig. 22 shows the SR with respect to the wobbling amplitude and indicates that the energy efficiency decreased as the amplitude increased. Figs. 23, 24, and 25 show stick diagrams of LCW under the condition of $K_a = 0.0$, 4.0, and 8.0, respectively. As shown in Fig. 23, the wobbling movement of the mass was synchronized with that of the torso mass, resulting in the slowest walking speed. In Figs 24 and 25, the wobbling movement of the mass is shown to be in antiphase with that of the torso mass. The largest amplitude can be seen in Fig. 25, and it corresponds to the fastest walking speed.

5.3. Radius of the arc-shaped feet

The bipedal robots used in this model were assumed to have arc-shaped feet, and we investigated the effects of changing their arc-radius. Fig. 26 shows that the walking speed increased as a function of this arc-radius. Fig. 27 shows the SR results with respect to the arc-radius: it can be seen that increasing the arc-radius under the conditions of the proposed method also improved the energy-efficiency. Furthermore, as was observed in a previous
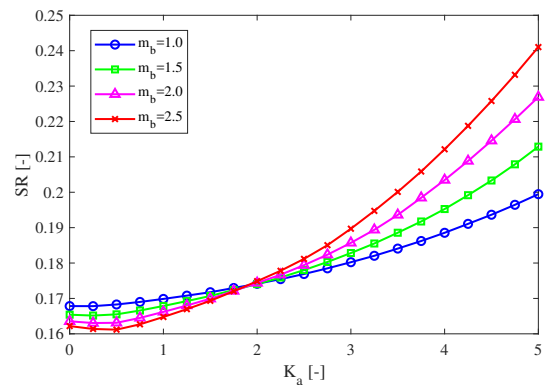

Fig. 22. SR with respect to amplitude of up-and-down motion

study of bipedal robots [5], the use of arc-shaped feet improved the energy efficiency and walking speed.
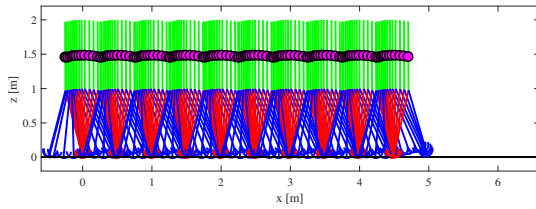
8

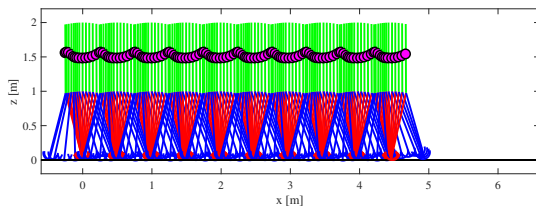**Fig. 23.** Stick diagram of LCW: $K_a = 0.0$
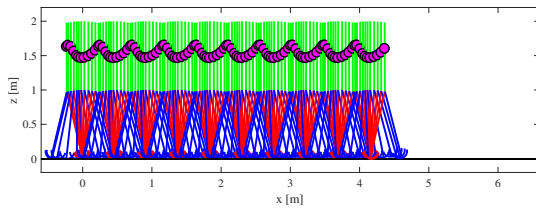

Fig. 24. Stick diagram of LCW: $K_a = 4.0$
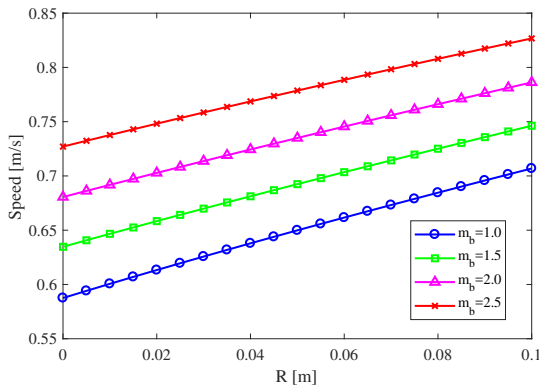

Fig. 25. Stick diagram of LCW: $K_a = 8.0$

Fig. 26. Walking speed with respect to arc-radius

6. IMPROVING THE WALKING PERFORMANCE BY USING A SPRING

We have demonstrated that fast level ground walking can be realized as a result of using the proposed control method. We also considered that the energy efficiency could be improved by incorporating a spring. In this section, we examine the effects of incorporating a spring
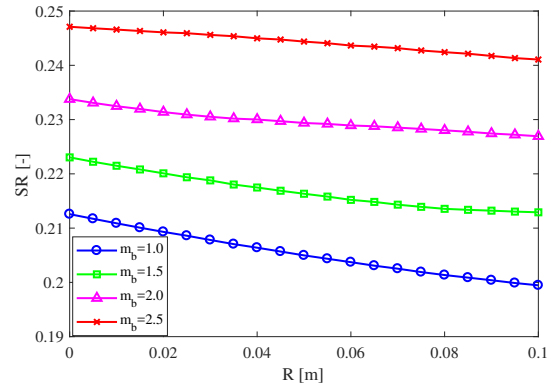

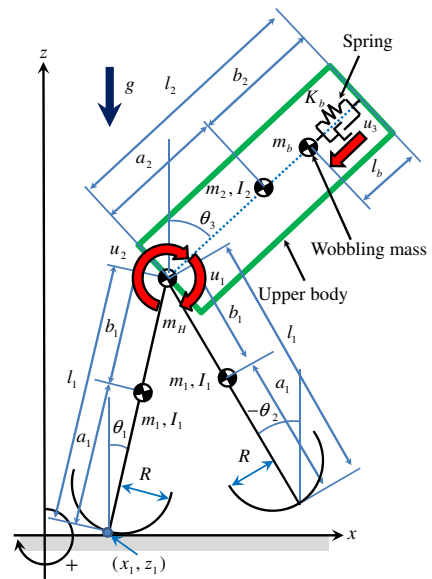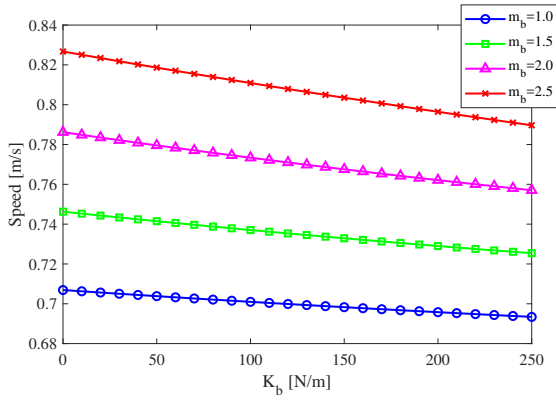**Fig. 27.** SR with respect to arc-radius

Fig. 28. Bipedal robot model with a spring and an actively controlled wobbling mass

on level ground walking with a wobbling mass. Fig. 28 shows the bipedal robot model with a spring and an actively controlled wobbling mass. The spring force is given by

$$f_b = -K_b(l_b - l_0), \quad \dots \dots \dots \dots \dots (32)$$

where K_b is the spring constant and l_0 is the natural spring length. Fig. 29 shows the walking speed with respect to the spring constant. Fig. 30 shows the SR results with respect to the spring constant. We see that the walking speed slightly decreases when the spring constant increases. However, the SR were convex downward and we can see that minimum value at the specific spring constant in each case.

Fig. 31 shows the walking speed with respect to the natural angular frequency. Fig. 32 shows the SR results with respect to the natural angular frequency. It can be seen that the walking speed slightly decreases when the natural

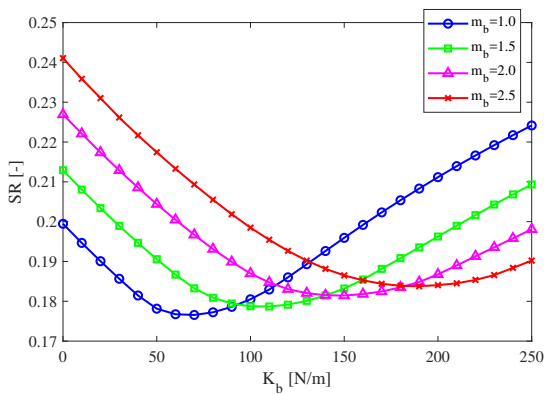**Fig. 29.** Walking speed with respect to spring constant

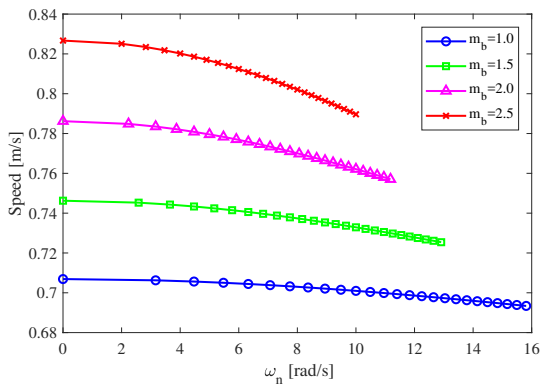**Fig. 30.** SR with respect to spring constant

Fig. 31. Walking speed with respect to natural angular frequency

angular frequency increases. However, the SR improves when the natural angular frequency ($\omega_n = \sqrt{K_b/m_b}$) is approximately 8.5 rad/s. Thus, we should design the wobbling mass and adjust the spring constant to satisfy $\omega_n \approx 8.5$ rad/s.

Fig. 32. SR with respect to natural angular frequency

7. CONCLUSION AND FUTURE WORK

In this study, we developed a novel fast walking method that entails the installation of an up-and-down wobbling mass in the torso and have validated its effectiveness through numerical simulation. We mathematically analyzed the gait cycle of a bipedal robot equipped with such a wobbling mass to clarify the mechanism by which the observed increase in speed was achieved. Based on the results of analysis, the wobbling movement of the mass in antiphase with that of the torso mass generated a virtual ankle torque, thereby generating a propulsive force that propels the robot forward. Our proposed mechanism can be used to further increase the speed of a limit cycle walker. Moreover, the walking speed of bipedal robots with dual-arm can be improved by arm-swinging movement based on the propulsive effects due to the up-and-down of a wobbling mass [16]. In the future, we want to develop a bipedal robot with a wobbling mass and verify the effectiveness of our control method by performing walking experiments. Additionally, we intend to develop a derivation method for the analytical solution of our model.

References:
[1] "PETMAN, " Supporting Online Materials.
[2] "Cassies, " Supporting Online Materials.
[3] T.McGeer, "Passive dynamic walking," The International Journal of Robotics Research, vol.9, no.2, pp.62–82,1990.
[4] S. H. Collins and A. Ruina, "A bipedal walking robot with efficient and human-like gait, " in Proc. IEEE International Conference on Robotics and Automation (ICRA), 2005, pp. 1983–1988.
[5] F. Asano and Z. W. Luo, "Efficient dynamic bipedal walking using effects of semicircular feet," Robotica, vol.29, no.3, pp.351–365, 2011.
[6] F. Asano and Z. W. Luo, "Energy-efficient and high-speed dynamic biped locomotion based on principle of parametric excitation, " IEEE Transactions on Robotics, vol.24, no.6, pp.1289–1301, 2008.

[7] Y. Banno, K. Taji, Y. Harata, and K. Seta, "A modied kneed biped real robot based on parametric excitation principle, " Automation Control and Intelligent Systems, vol. 2, no. 5, pp. 93–99, 2014.

[8] D. Hobbelen and M. Wisse,, "Controlling the walking speed in limit cycle walking, " The International Journal of Robotics Research, vol. 27, no. 9, pp. 989–1005, 2008.

[9] Y. Hanazawa, H. Suda, Y. Iemura, and M. Yamakita, "Active walking robot mimicking at-footed passive dynamic walking," in Proc. IEEE International Conference on Robotics and Biomimetics (RO-BIO), pp. 1281–1286, 2012.

[10] Y. Hanazawa and F. Asano, "Asymmetric swing-leg motions for speed-up of biped walking," Journal of robotics and mechatoronics, vol. 29, no. 3, pp. 490–499, 2017.

[11] R. Bao and T.Geng, "Fast walking with rhythmic sway of torso in a 2D Passive Ankle Walker," in Proc. IEEE/RSJ International Conference on Intelligent Robots and Systems (IROS), pp. 4363–4368, 2018.

[12] D. Hobbelen and M. Wisse,, "Limit cycle walking, " Humanoid Robots, Human-like Machines, pp. 277–294, 2007.

[13] L. Rome, L. Flynn, and T. Yoo, "Biomechanics: Rubber bands reduce the cost of carrying loads," Nature, vol. 444, no. 7122, pp. 1023–1024, 2006.

[14] D. Tanaka, F. Asano, and I. Tokuda, "Gait analysis and efficiency improvement of passive dynamic walking of combined rimless wheel with wobbling mass," in Proc. IEEE/RSJ International Confer- ence on Intelligent Robots and Systems (IROS), pp. 151–156, 2012.

[15] S. H. Collins , P. G. Adamczyk, and A. D. Kuo, "Dynamic arm swinging in human walking", in Proc. the Royal Society B: Biological Sciences, vol. 276, no. 1673 pp. 3679–3688, 2009.

[16] Y. Hanazawa and F. Asano, "High-speed biped walking using swinging-arms based on principle of up-and-down wobbling mass." in Proc. IEEE International Conference on Robotics and Automation (ICRA), pp. 5191–5196, 2015.

Name:
Your Name

Affiliation:
Your Institute

Address:
Address of Your Institute
Brief Biographical History:
Your History
Main Works:
● Your Works
Membership in Academic Societies:
● Your Learned Societies

Name:
Your Name

Affiliation:
Your Institute

Address:
Address of Your Institute
Brief Biographical History:
Your History
Main Works:
● Your Works
Membership in Academic Societies:
● Your Learned Societies

Name:
Your Name

Affiliation:
Your Institute

Address:
Address of Your Institute
Brief Biographical History:
Your History
Main Works:
● Your Works
Membership in Academic Societies:
● Your Learned Societies

Name:
Your Name

Affiliation:
Your Institute

Address:
Address of Your Institute
Brief Biographical History:
Your History
Main Works:
● Your Works
Membership in Academic Societies:
● Your Learned Societies